S & M 4189

Effects of Annealing Temperature and Sputtering Power on the Optical and Electrical Properties of Transparent Conductive Zinc Oxide Films Doped with Titanium

Wen-Nan Wang, Yun-Hsin Cheng, Hsin-Yun Chiu, An-Tai Chiu, and Tao-Hsing Chen*

Department of Mechanical Engineering, National Kaohsiung University of Science and Technology, No. 415, Jiangong Rd., Sanmin Dist., Kaohsiung City 807618, Taiwan

(Received August 25, 2025; accepted September 29, 2025)

Keywords: ZnO:Ti, electrical property, sputtering, optical property, annealing

In this study, we investigated the optical and electrical properties of transparent conductive zinc oxide (ZnO) thin films doped with titanium (Ti) deposited through radio frequency (RF) sputtering at different annealing temperatures and sputtering powers. The ZnO:Ti thin films exhibited the lowest resistivity of 1.60×10^{-3} Ω -cm, a high transmittance of 89%, and the optimal figure of merit (FOM) of 9.31×10^{-8} Ω^{-1} when sputtered at 100 W for 30 min and annealed at 500 °C. The scanning electron microscopy of the films' surface morphology revealed that higher annealing temperatures promoted grain growth.

1. Introduction

Thin films are a unique class of materials widely used in solar cells, liquid crystal displays, and sensors. For example, the transparent conductive oxide (TCO) film is a critical optoelectronic material exhibiting high electrical conductivity and excellent transmittance in the visible wavelength range; therefore, it is widely used in the optoelectronics industry. The advent of TCOs represents a significant scientific breakthrough as transparent materials such as glass are generally insulating, whereas conductive materials such as metals or graphite are typically opaque.^(1–5)

TCOs have become one of the most functional thin films by combining electrical conductivity with optical transmission. In particular, indium tin oxide (ITO) thin films have broad applications because of their superior conductivity and transmission. $^{(6-8)}$ These films achieve a transmittance exceeding 85% in the visible range, demonstrating a lower resistivity (10^{-5} to 10^{-3} Ω -cm), a higher hardness, and a higher wear resistance than metal thin films. In addition, they can be easily etched into electrode patterns and exhibit a high microwave attenuation (approximately 85%). However, they have several limitations. For example, metallic indium (In) precipitates from the films under reducing atmospheres leading to toxicity. In is a rare metal with limited global supply; thus, manufacturing optoelectronic devices containing ITO thin films has become prohibitively

*Corresponding author: e-mail: thchen@nkust.edu.tw https://doi.org/10.18494/SAM5890

expensive. Therefore, the search for alternative transparent conductive films is ongoing. Zinc oxide (ZnO) has emerged as a promising replacement but the electrical properties of undoped ZnO thin films are inherently unstable, largely because the surface adsorption of oxygen atoms introduces surface charges. (9-12) Titanium (Ti) doping was performed in this study to improve the films' electrical properties. (13,14)

The annealing process leads to more oxygen vacancies, thereby increasing the carrier concentration and conductivity of ZnO films, (15-18) but the sputtering parameters such as the partial pressure of oxygen and sputtering power must be carefully controlled. Moreover, numerous researchers have focused on the role of the substrate temperature during sputtering and the annealing temperature after sputtering in the electrical properties of the films. Several researchers have also proposed that factors in addition to work function and thermal stability—e.g., raw material costs and etching processes—must be taken into consideration when evaluating the performance of TCOs. In this study, ZnO acted as the sputtering target, which was doped with Ti as an aliovalent impurity. The ionic radius of Ti⁴⁺ (0.68 nm) is comparable to that of Zn²⁺ (0.74 nm), thereby minimizing lattice distortion when Zn²⁺ was substituted by Ti⁴⁺, potentially contributing two electrons to enhance the film conductivity.

2. Experimental Methods and Procedures

Corning quartz glass was cleaned of dust and organic contaminants using deionized water and acetone under ultrasonic agitation before oven drying at 90 °C for 30 min. The sputtering of ZnO:Ti (95:5 at%) was performed using a radio frequency (RF) sputtering system (Ishien Vacuum) in vacuum with specific changes in sputtering power and time. The sputtering work distance was 60 mm with a fixed bias of 6 mTorr, a gas flow rate of 15 sccm, an ambient gas of Ar, and a sputtering time of 30 min. Furthermore, the sputtering powers were 60, 80, and 100 W. Finally, the deposited dual-layer films were annealed in vacuum at 200, 300, 400, and 500 °C with each temperature maintained for 5 min in a vacuum annealing furnace. The transmittance and conductivity of the films were then measured using a spectrophotometer and a Hall effect measurement system, respectively. The phase composition of the films was analyzed by X-ray diffraction (XRD), and their surface morphology was examined by SEM.

3. Results and Discussion

3.1 XRD characterization

The XRD patterns of ZnO:Ti thin films sputtered at 60 W (Fig. 1) revealed that the films remained amorphous from the as-deposited state up to annealing at 400 °C with no crystalline phases observed. Crystallization did not occur until annealing at 500 °C. There were no Tirelated peaks due to the uniform distribution of Ti ions within the ZnO lattice. ZnO (002) diffraction peaks appeared after annealing at 400 °C and when thin films were sputtered at 80 W (Fig. 2) and 100 W (Fig. 3). It is different for films sputtered at 60 W.

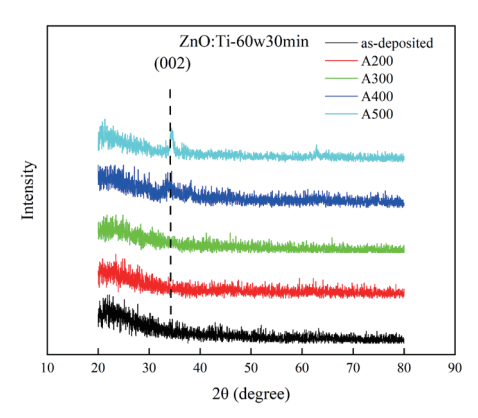


Fig. 1. (Color online) XRD patterns of ZnO:Ti thin films sputtered at 60 W and annealed at different temperatures.

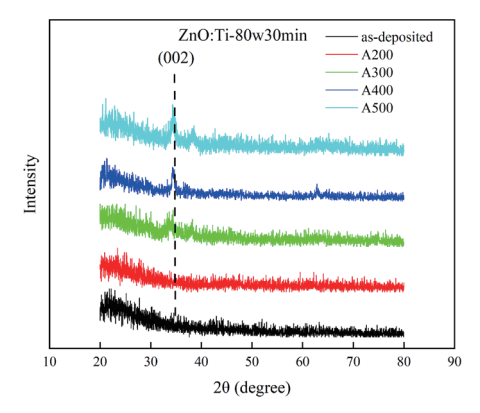


Fig. 2. (Color online) XRD patterns of ZnO:Ti thin films sputtered at 80 W and annealed at different temperatures.

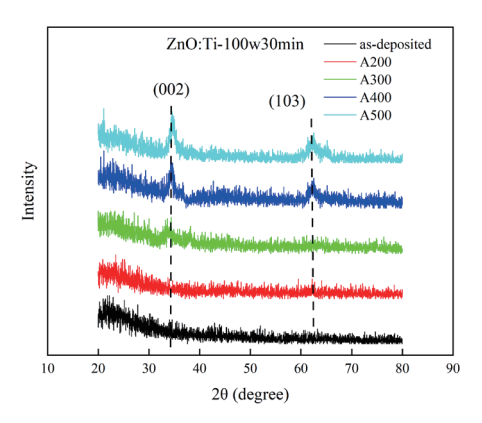


Fig. 3. (Color online) XRD patterns of ZnO:Ti thin films sputtered at 100 W and annealed at different temperatures.

3.2 Electrical properties of ZnO:Ti thin films

A Hall effect measurement system was used to estimate the mobility, carrier concentration, and resistivity of the conductive ZnO:Ti thin films (Tables 1–3). The lowest resistivity of $3.38 \times 10^{-3} \Omega$ -cm was achieved after annealing at 500 °C and the sputtering power was 60 W. Notably, when the sputtering power was increased to 80 and 100 W, the lowest resistivity was

7,0,Ti 60 W 20 min
Electrical properties of ZnO:Ti thin films sputtered at 60 W and annealed at different temperatures.
Table 1

ZnO:Ti 60 W 30 min			
Annealing temperature (°C)	Resistivity (Ω-cm)	Mobility (cm ² /V-s)	Carrier concentration (cm ⁻³)
As-deposited	5.19×10^{-2}	14	2.5×10^{16}
200	8.78×10^{-3}	19	3.75×10^{17}
300	5.53×10^{-3}	21	8.75×10^{17}
400	4.07×10^{-3}	30	9.2×10^{17}
500	3.38×10^{-3}	35	9.7×10^{17}

Table 2 Electrical properties of ZnO:Ti thin films sputtered at 80 W and annealed at different temperatures.

ZnO:Ti 80 W 30 min			
Annealing temperature (°C)	Resistivity (Ω-cm)	Mobility (cm ² /V-s)	Carrier concentration (cm ⁻³)
As-deposited	3.11×10^{-2}	20	4.5×10^{17}
200	5.77×10^{-3}	23	5.3×10^{17}
300	4.04×10^{-3}	28	6.9×10^{17}
400	3.71×10^{-3}	33	9.3×10^{17}
500	2.85×10^{-3}	37	1.2×10^{18}

Table 3 Electrical properties of ZnO:Ti thin films sputtered at 100 W and annealed at different temperatures.

ZnO:Ti 100 W 30 min			
Annealing temperature (°C)	Resistivity (Ω-cm)	Mobility (cm ² /V-s)	Carrier concentration (cm ⁻³)
As-deposited	2.50×10^{-2}	21	5.6×10^{17}
200	4.49×10^{-3}	28	7.2×10^{17}
300	3.51×10^{-3}	32	9.3×10^{17}
400	2.58×10^{-3}	38	1.4×10^{18}
500	1.60×10^{-3}	40	2.2×10^{18}

also observed at the same annealing temperature, decreasing further to 2.85×10^{-3} and 1.60×10^{-3} Ω -cm, respectively. Therefore, the films exhibited the highest conductivity when sputtered at 100 W.

3.3 Transmittance of ZnO:Ti thin films

The transmittance of ZnO:Ti thin films sputtered at different powers and annealed at different temperatures decreased as the sputtering power increased (Figs. 4–8). This inverse relationship was attributed to the corresponding increase in film thickness with higher sputtering power, reducing the transmittance. Therefore, post-sputtering annealing was performed to improve the film transmittance. However, the transmittance did not significantly improve with annealing temperature, and in some cases, it decreased slightly. This was mainly due to the enhanced free carrier absorption increasing the film absorption in the visible and infrared regions, thereby reducing the film transmittance.

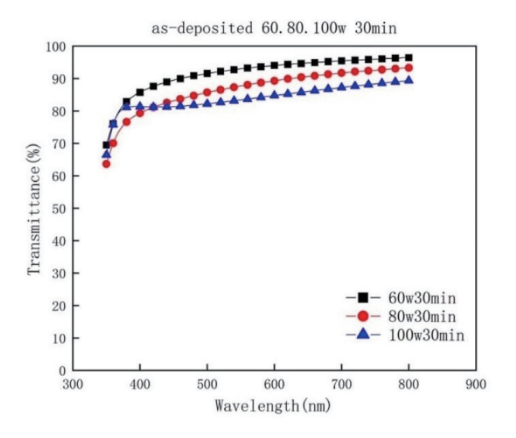


Fig. 4. (Color online) Transmittance of ZnO:Ti thin films in the as-deposited state.

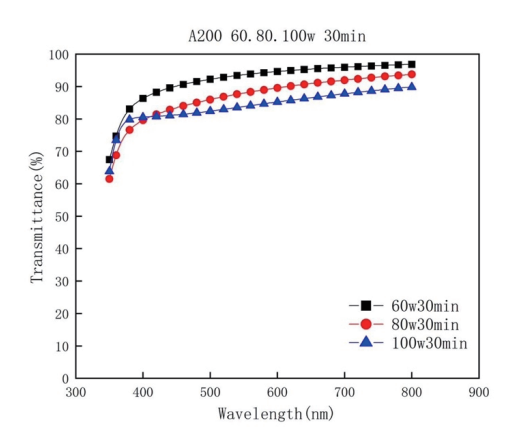


Fig. 5. (Color online) Transmittance of ZnO:Ti thin films annealed at 200 $^{\circ}$ C.

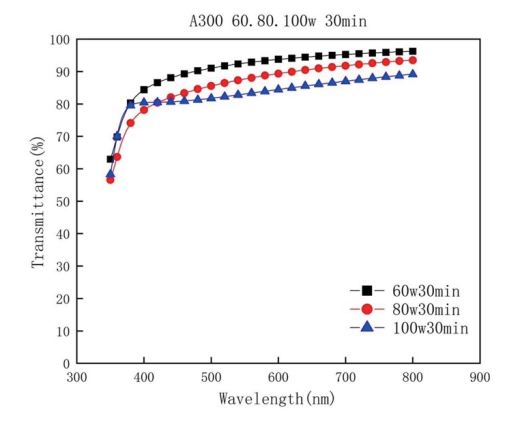


Fig. 6. (Color online) Transmittance of ZnO:Ti thin films annealed at 300 $^{\circ}\mathrm{C}.$

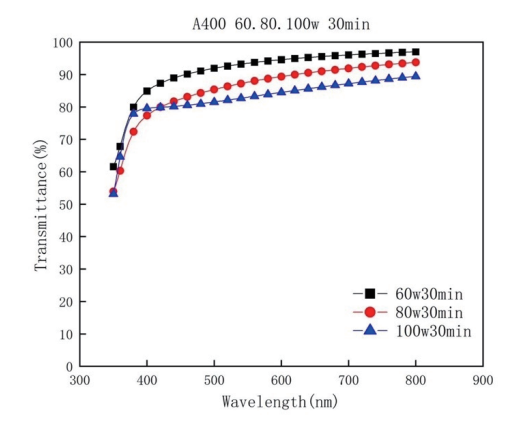


Fig. 7. (Color online) Transmittance of ZnO:Ti thin films annealed at 400 $^{\circ}\text{C}.$

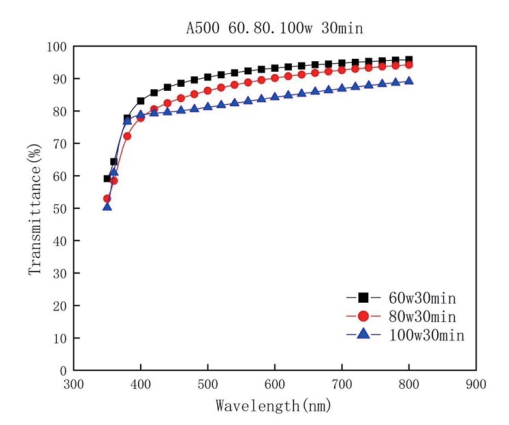


Fig. 8. (Color online) Transmittance of ZnO:Ti thin films annealed at 500 °C.

3.4 Figure of merit (FOM)

The quality of the transparent conducting films (TCFs) was evaluated on the basis of their FOM calculated as⁽²⁰⁻²²⁾

$$\varnothing_{TC} = \frac{T_{av}^{10}}{R_{sh}},\tag{1}$$

where T_{av} is the average optical transmittance and R_{sh} is the sheet resistance expressed in Ω^{-1} . In this equation, the tenth power of transmittance is directly proportional to the FOM, indicating the significance of transmittance for the FOM (see Tables 4–6). Achieving a higher FOM necessitates maintaining high transmittance while reducing resistance. Indeed, at the sputtering powers of 60, 80, and 100 W, the optimal FOMs of 4.46×10^{-9} , 1.91×10^{-9} , and $9.31 \times 10^{-8} \Omega^{-1}$, respectively, were obtained at the annealing temperature of 500 °C. However, the highest FOM occurred at the sputtering power of 100W.

Table 4 FOMs of ZnO:Ti thin films sputtered at 60 W and annealed at different temperatures.

$FOM, \varnothing_{\mathit{TC}}(\Omega^{-1})$		
Annealing temperature (°C)	ZnO:Ti (60 W)	
As-deposited	1.31×10^{-9}	
200	4.09×10^{-10}	
300	4.26×10^{-10}	
400	7.87×10^{-10}	
500	4.46×10^{-9}	

Table 5 FOMs of ZnO:Ti thin films sputtered at 80 W and annealed at different temperatures.

$FOM, \varnothing_{\mathit{TC}}(\Omega^{-1})$		
Annealing temperature (°C)	ZnO:Ti (80 W)	
As-deposited	5.57×10^{-10}	
200	1.10×10^{-9}	
300	1.51×10^{-9}	
400	1.66×10^{-9}	
500	1.91×10^{-9}	

Table 6 FOMs of ZnO:Ti thin films sputtered at 100 W and annealed at different temperatures.

FOM, $\varnothing_{TC}(\Omega^{-1})$		
Annealing temperature (°C)	ZnO:Ti (100 W)	
As-deposited	2.49×10^{-10}	
200	4.60×10^{-9}	
300	3.09×10^{-9}	
400	2.77×10^{-9}	
500	9.31×10^{-8}	

3.5 Surface morphology

The SEM results of the surface morphology of the ZnO:Ti thin films (Figs. 9–11) revealed that the grain growth increased with annealing temperature at a constant sputtering power. Similarly, the grain growth increased slightly with sputtering power at a constant annealing temperature. Therefore, annealing temperature and sputtering power both promoted the film grain growth.

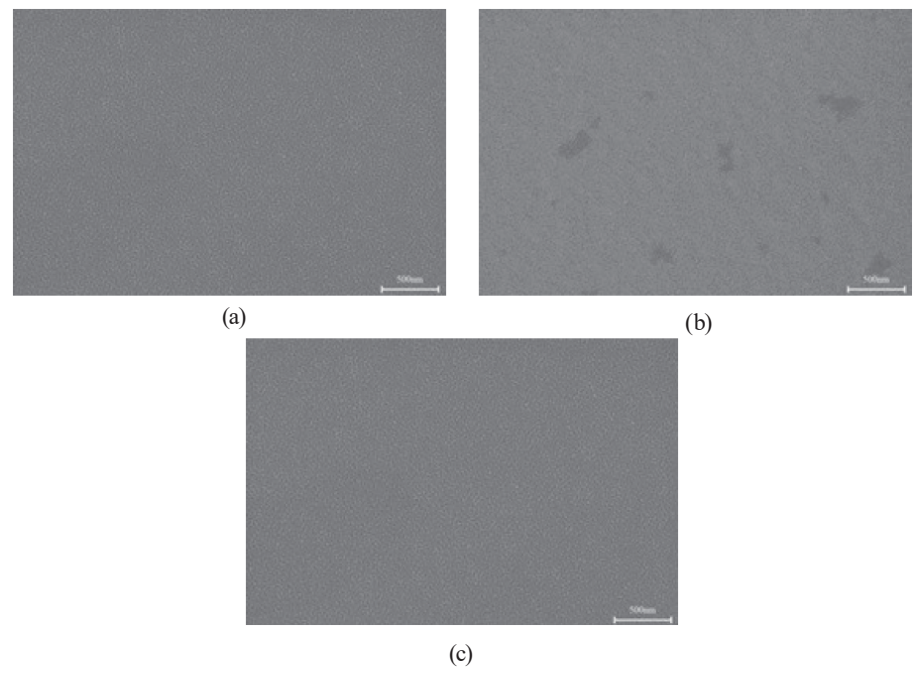


Fig. 9. Surface morphology of ZnO:Ti thin films sputtered at 60~W and annealed at different temperatures: (a) asdeposited, (b) 200~°C, and (c) 500~°C.

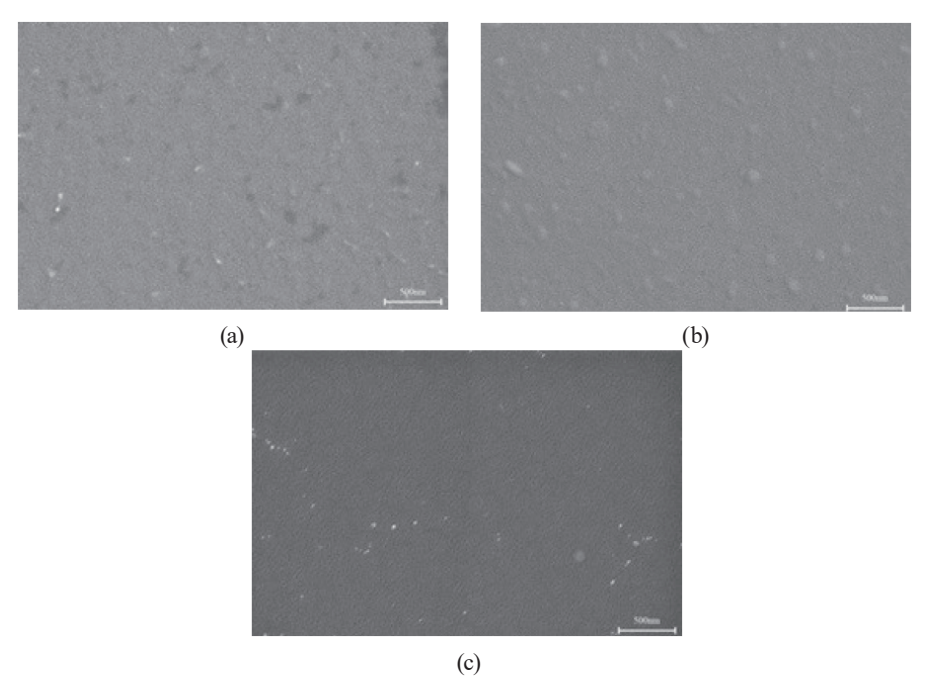


Fig. 10. Surface morphology of ZnO:Ti thin films sputtered at 80 W and annealed at different temperatures: (a) asdeposited, (b) $200 \,^{\circ}$ C, and (c) $500 \,^{\circ}$ C.

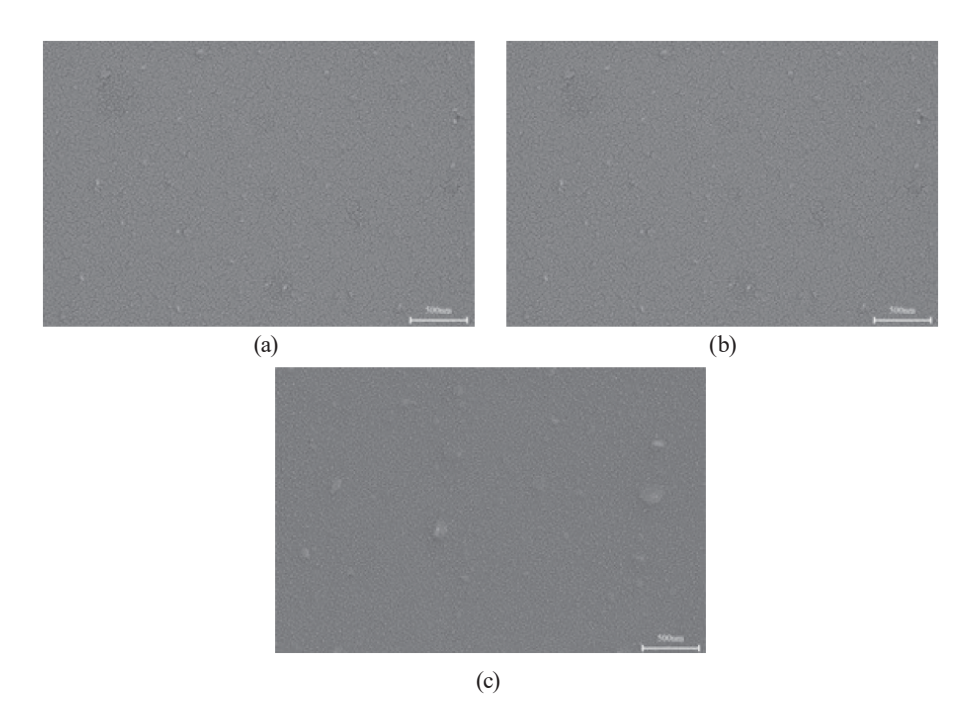


Fig. 11. Surface morphology of ZnO:Ti thin films sputtered at 100 W and annealed at different temperatures: (a) as-deposited, (b) 200 °C, and (c) 500 °C.

4. Conclusions

The ZnO:Ti thin films exhibited the lowest resistivities of 3.38×10^{-3} , 2.85×10^{-3} , and 1.60×10^{-3} Ω -cm at the sputtering powers of 60, 80, and 100 W, respectively, when the films were annealed at 500 °C. The optical transmittance of the films decreased as the sputtering power increased, with no significant improvement in transmittance when the annealing temperature increased owing to changes in carrier concentration. The films achieved optimal FOMs of 1.46×10^{-9} and 1.91×10^{-9} Ω at the sputtering powers of 60 and 80 W, respectively, when annealed at 500 °C. The optimal FOM of 9.31×10^{-8} Ω^{-1} was achieved after annealing at 500 °C at the sputtering power of 100 W, resulting in the lowest resistivity and high transmittance. The higher sputtering power and annealing temperature promoted grain growth. The results presented in this paper can be applied to optical sensors and materials.

Acknowledgments

This study was completed as part of Research Project MOST111-2628-E-992-001-MY2, which is supported by the National Science and Technology Council of Taiwan. The authors would like to express their gratitude to the National Science and Technology Council for its support, which enabled the smooth completion of this research. The authors also gratefully acknowledge the use of EM000700 of MOST 113-2731-M-006-001 belonging to the Core Facility Centre of National Cheng Kung University.

References

- 1 W. N. Wang, T. D. Chang, and T. H. Chen: Sens. Mater. **36** (2024) 3757. https://doi.org/10.18494/SAM5049
- C. H. Yu, S. T. Wicaksono, S. T. Wang, and T. H. Chen: Sens. Mater. 37 (2025) 1825. https://doi.org/10.18494/SAM5316
- 3 A. X. Wang and W. C. Hsu: Appl. Phys. Lett. 124 (2024) 060503. https://doi.org/10.1063/5.0179441
- 4 H. Ferhati and F. Djeffal: J. Comput. Electron. 19 (2020) 815. https://doi.org/10.1007/s10825-020-01459-9
- 5 S. Singh, V. Sharma, and K. Sachdev: J. Mater. Sci. **52** (2017) 11580. https://doi.org/10.1007/s10853-017-1328-7
- 6 K. H. Choi, J. Y. Kim, Y. S. Lee, and H. J. Kim: Thin Solid Films 341 (1999) 152. https://doi.org/10.1016/S0040-6090(98)01556-9
- 7 A. K. Sahoo, W. C. Au, and C. L. Pan: Coating 14 (2024) 895. https://doi.org/10.3390/coatings14070895
- 8 S. Liu, X. Xu, and J. Jiang: Ceramics Int. **50** (2024) 47649. https://doi.org/10.1016/j.ceramint.2024.09.110
- 9 T. H. Chen and C. L. Yang: Opt. Quantum Electron. 48 (2016) 533. https://doi.org/10.1007/s11082-016-0808-3
- 10 M. Y. Yen, T. H. Chen, P. H. Lai, S. L. Tu, and Y. H. Shen: Sens. Mater. 33 (2021) 3941. https://doi.org/10.18494/SAM.2021.3706
- T. Y. Tsai, C. J. Liu, T. D. Chang, S. L. Tu, and T. H. Chen: Sens. Mater. 36 (2024) 671. https://doi.org/10.18494/SAM4684
- 12 E. Ş. Tüzemen, S. Eker, H. Kavak, and R. Esen: Appl. Sur. Sci. **255** (2009) 2195. https://doi.org/10.1016/j.apsusc.2009.01.078
- 13 C. F. Liu, T. H. Chen, and Y. S. Huang: Sens. Mater. 32 (2021) 2321. https://doi.org/10.18494/SAM.2020.2867
- 14 Y. M. Lu, C. M. Chang, S. I. Tsai, and T. S. Wey: Thin Solid Films 447–448 (2004) 56. https://doi.org/10.1016/j.tsf.2003.09.022
- 15 Y. C. Chang, T. H. Chen, T. D. Chang, S. L. Tu, and Y. H. Shen: Sens. Mater. 35 (2023) 2871. <u>https://doi.org/10.18494/SAM4354</u>
- 16 T. H. Chen, T. C. Cheng, and Z. R. Hu: Microsyst. Technol. 19 (2013) 1787. https://doi.org/10.1007/s00542-013-1837-5
- 17 R. M. Al Jarrah, E. M. Kadhem, and A. H. O. Alkhayatt: Appl. Phys. A 128 (2021) 527. https://doi.org/10.1007/s00339-022-05659-x
- 18 A. Alshoaibi: Inorganics **12** (2024) 236. https://doi.org/10.3390/inorganics12090236
- 19 M. Sultan and N. Sultana: J. Electr. Electron. Sys. 4 (2015) 1000160. https://doi.org/10.4172/2332-0796.1000160
- 20 C. F. Liu, S. C. Shi, T. H. Chen, and G. L. Guo: Sens. Mater. 34 (2022) 4127. https://doi.org/10.18494/SAM4133
- 21 D. Kim: Mater. Lett. **64** (2010) 668. https://doi.org/10.1016/j.matlet.2009.12.032
- 22 C. Y. Lin, T. H. Chen, S. L. Tu, Y. H Shen, and J. T. Huang: Opt. Quant. Electron. 50 (2018) 169.

About the Authors



Wen-Nan Wan received his M.S. degree from Chi-Yi University, Taiwan, in 2022. Currently, he is a Ph.D. student at the Department of Mechanical Engineering, National Kaohsiung University of Science and Technology. Since 2010, he has been the general manager of Shieh Ho Tien Enterprise Co., Ltd. His research interests include optical materials, heat transfer, fluid sensors, and pressure sensors.



Yun-Hsin Cheng received her B.S. degree from National Kaohsiung University of Science and Technology, Taiwan, where she is currently studying for her M.S. degree. Her research interests include TCO thin films, materials engineering, and sensors.



Hsin-Yun Chiu received her B.S. degree from National Kaohsiung University of Science and Technology, Taiwan, where she is currently studying for her M.S. degree. Her research interests include TCO thin films, materials engineering, and sensors.



An-Tai Chiu received his B.S. degree from National Kaohsiung University of Science and Technology, Taiwan. At present, he is serving in the military. His research interests include TCO thin films, materials engineering, and sensors.



Tao-Hsing Chen received his B.S. degree from National Cheng Kung University, Taiwan, in 1999, and his M.S. and Ph.D. degrees from the Department of Mechanical Engineering, National Cheng Kung University, in 2001 and 2008, respectively. From August 2008 to July 2010, he was a postdoctoral researcher at the Centre for Micro/Nano Science and Technology, National Cheng Kung University. In August 2010, he became an assistant professor at National Kaohsiung University of Applied Sciences (renamed National Kaohsiung University of Science and Technology), Taiwan. Since 2016, he has been a professor at National Kaohsiung University of Science and Technology. His research interests include metal materials, TCO thin films, thermal sensors, and photosensors. (thchen@nkust.edu.tw)